# AIAA 93-4328
# Direct Computation of the Sound Generated by a Two-Dimensional Shear Layer

T. Colonius, S.K. Lele, and P. Moin
Stanford University
Stanford, CA

**15th AIAA**
**Aeroacoustics Conference**
October 25-27, 1993 / Long Beach, CA

# DIRECT COMPUTATION OF THE SOUND GENERATED BY TWO-DIMENSIONAL SHEAR LAYER

Tim Colonius *
Sanjiva K. Lele **
Parviz Moin ***
Department of Mechanical Engineering
Stanford University, Stanford, CA 94305-3030

## Abstract

The sound generated by a two dimensional shear layer is investigated by Direct Numerical Simulation (DNS) of the compressible Navier-Stokes equations. A high-order-accurate numerical scheme and non-reflecting boundary conditions are used to accurately compute both the near field hydrodynamics and the acoustic waves produced by the layer. The directly computed acoustic field shows that the acoustic waves which are generated at the fundamental frequency (most unstable mode), and its first two sub-harmonics, originate near the region where the instability wave at these frequencies saturate, i.e. the region where the layer rolls up into vortices for the fundamental frequency, and the first two vortex pairings for the sub-harmonics. The sound generated by the pairings is most intense in the downstream direction, indicating a superdirective acoustic source.

## 1.0 Introduction

The derivation of acoustic analogies is based on a rearrangement of the conservation equations describing mass, momentum and energy in the flow field into a wave propagation operator and a source term. For low Mach number flows with compact vorticity fields, acoustic analogies can be rigorously derived using matched asymptotic expansions (Kambe[1]). However, most flows of practical interest, including jets, mixing layers, and boundary layers, do not possess compact vorticity fields and the rearrangement of the equations leading to an acoustic analogy is ambiguous. It is possible to make some progress by performing asymptotic expansions of the disturbances to a unidirectional transversely sheared flow (Goldstein[2]). This results in an acoustic analogy similar to the one proposed by Lilley[3]. Ultimately, however, nonlinear effects which dominate the hydrodynamics of such disturbances preclude an unambiguous analytical solution of the asymptotic expansion. In that case one must regard the source term as independently known, determined either by experiment or computational fluid dynamics, and it cannot be determined *a priori* how accurate is the estimate for the acoustic field thus produced.

To address these issues it becomes necessary to have access to the "exact" far-field sound and the unsteady hydrodynamic flow field. This information can be obtained by directly solving the compressible flow equations in both regions. Such a computation must overcome a number of difficulties before it can be regarded as reliable. Typical acoustic fluctuations have very small energy compared to near field vorticity fluctuations and thus a very accurate numerical scheme which minimizes phase and amplitude errors over a wide range of scales is necessary. Furthermore, the computational domain must be large in order to capture several wavelengths of the generated sound waves. Finally, boundary conditions which minimize numerical reflection of both outgoing acoustic waves and vortical structures are necessary.

We have developed such a numerical scheme, and validated it on a number of model problems. The scheme was presented in detail in Colonius, Lele and Moin[4]. It was found that by using a 6th order accurate compact finite difference scheme coupled with explicit 4th order Runge Kutta time advancement, numerical discretization errors can be made small enough to accurately represent the generated acoustic waves in the computation. The generation of sound by a co-rotating vortex pair (with a compact vorticity field) was computed by Mitchell, Lele and Moin[5] using the current numerical scheme. Good agreement was observed between the computed result and analytical predictions. The scattering of waves by a single vortex was also computed (Colonius *et al.*[6]) and found to be in good agreement with experiments and theory. Furthermore, we have developed an absorbing downstream boundary condition[4] which allowed large scale vortex structures (associated with the roll up of the most unstable mode in a 2-d mixing layer) to exit the domain smoothly, reducing the magnitude of spurious reflections by3 orders of magnitude compared to linear non-reflecting outflow boundary conditions, such as those proposed by Giles[7].

In the current study, the scheme is used to compute the sound generated by a two dimensional mixing layer. The computation is restricted to two dimensions to allow a very large computational domain which contains

* Student Member, AIAA
** Also with Department of Aeronautics and Astronautics, Stanford University
*** Also with NASA Ames, Associate Fellow AIAA

a significant portion of the generated acoustic field. The mixing layer is chosen since the low frequency sound in jets is thought to be a result of large scale structures which are created by instabilities in the initial shear layers.

## 2.0 Numerical Method

The two dimensional compressible Navier-Stokes Equations, plus conservation of mass and energy and the perfect gas law are solved in conservative form on a Cartesian mesh. The numerical method relies on 6th order accurate compact finite difference scheme (Lele[8]) for spatial derivatives and an explicit 4th order Runge Kutta time advancement, in order to accurately resolve both hydrodynamic fluctuations and acoustic waves. The scheme has very low numerical dissipation and dispersion. A schematic diagram of the computational domain used for the mixing layer is shown in Figure 1. The streamwise and spanwise coordinates, $x$ and $y$ respectively, have been normalized with respect to the initial vorticity thickness of the layer, $\delta$, at $x = 0$. The domain extends to $285\delta$ in the streamwise direction, and to $\pm 200\delta$ in the normal direction. The streamwise and normal directions are discretized with 2300 and 847 grid points respectively. Non-reflecting boundary conditions are used at the inflow boundaries (the top and bottom boundaries are also inflow boundaries due to entrainment by the layer), and a combination of non-reflecting boundary conditions and sponge outflow are used at the downstream outflow boundary. These boundary condtions and the numerical scheme are discussed in detail by Colonius *et al.*[4]

The Mach numbers of the high and low speed streams forming the mixing layer are .5 and .25 respectively. Due to the low Mach number, the domain is quite large to include many wavelengths of the generated sound. The initial condition for the computation is a solution of the compressible steady boundary layer equations. This solution is found using the scheme described by Sandham and Reynolds[9]. The Reynolds number, based on the velocity, density and viscosity of the high speed stream and the initial vorticity thickness of the layer is 500, and the temperature ratio across the layer is 1. The Prandtl number is 1 and molecular properties are taken to be constant.

In order to study the sound generated by large scale structures in the mixing layer, the layer is forced at its most unstable frequency and several of its sub-harmonics. This causes the layer to roll up and pair in an organized manner. This allows the sound generated by the mixing layer to be investigated without the additional complication of fine grained turbulence.

Ho*et al.*[10]have shown that by forcing a two dimensional layer at its fundamental and first $m$ sub-harmonics, the layer becomes phase correlated as far downstream as the $m+1$st pairing location. Thus by forcing the layer at these frequencies the layer becomes approximately periodic in time at streamwise locations in the region of phase correlation.

This periodic nature causes the roll up and subsequent pairings to occur at fixed streamwise locations. In terms of the generated acoustic field, this has the important consequence of causing the acoustic sources at a particular frequency to be stationary. Laufer and Yen[11] measured the acoustic field produced by a forced low Mach number jet and verified that the acoustic sources were indeed stationary, and related directly to the pairing of vortices in the initial shear layers. The highly organized time periodic flow which results from the forcing is advantageous from a computational point of view (over layers with higher degrees of randomness or phase decorrelation) since it allows the frequency spectrum of the various flow quantities (including the acoustic sources) to be determined by Discrete Fourier Transforms (DFT) over a single period of the lowest frequency in the periodic signal. This longest period is still much shorter than the lowest period for a flow which has a more random occurrence of roll ups and pairings. Thus the computational expense is much lower.

The computations are forced at the inflow ($x = 0$) with eigenfunctions (linearized disturbances) from the inviscid parallel shear flow corresponding to the viscous flow at $x = 0$. The spatial instability eigenfunctions are determined by the method given by Sandham*et al.*[10]which utilizes a 4th order Runge Kutta shooting scheme. The eigenfunctions are periodic in time, and cause disturbances which both oscillate and grow exponentially in the streamwise direction. The fundamental frequency is that for which the spatial growth rate is a maximum. $\omega_{fund.} = .63U_1/\delta$ where $U_1$ is the velocity of the high speed stream and $\delta$ is the initial vorticity thickness of the layer.

The layer is also forced with the first three subharmonics of the fundamental frequency. The amplitude of each disturbance is normalized such that its maximum streamwise velocity is .001 times the streamwise velocity of the high speed stream. The phase of the disturbances is chosen so that the streamwise location where the pairing occurs is minimized (with respect to the inflow).

## 3.0 DNS Results

### *3.1 Near Field Hydrodynamics*

We first examine the near field hydrodynamics of the computed mixing layer. Of primary interest is the extent to which the mixing layer becomes periodic in time when forced as indicated in the last section. Figure 2 shows time traces of the streamwise velocity at $y = 0$ in the mixing layer for various streamwise locations downstream of the inflow boundary. The time is normalized with respect to the period of the 3rd sub-harmonic frequency, $T$, where $T = 16\pi/\omega_f$.

At the first location, $x = 0$ (inflow), the forcing is felt instantly, and the signal quickly becomes periodic. All components of the forcing are felt equally at $x = 0$. At $x = 45.0$, the signal is undisturbed until the initial start-up forcing reaches the location, at around $t = 100$. After that time the fundamental frequency and its first sub-harmonic clearly dominate the signal. By $x = 100$, the signal evidently contains many higher frequencies, but is dominated by the 1st and 2nd sub-harmonics. By $x = 200$ the influence of the first sub-harmonic has been diminished, the 2nd sub-harmonic dominates, and the 3rd sub-harmonic is beginning to have an influence. By $x = 285$, the 3rd sub-harmonic dominates. Figure 2 shows that the layer has indeed become very nearly periodic in time over the entire length of the domain by about $t = 1000$. A careful examination of the plots also indicates that there is at least some energy in frequencies lower than the 3rd sub-harmonic, but it appears to be small.

In Figure 3 contours of the instantaneous vorticity in the sheared region are plotted at a time after the layer has become nearly periodic. Note that the scale in the normal direction has been expanded by a factor of 2.5 in the plot. The vorticity contours clearly show the layer rolling up into vortices, and two subsequent pairings. Note that the third sub-harmonic does not saturate (i.e. cause a third pairing) within the computational domain.

It is also useful to have access to the DNS results in the frequency domain to examine the growth and decay of the instability waves, and to isolate the acoustic waves at a particular frequency. Since the flow becomes essentially periodic in time, we can perform a Discrete Fourier Transform in time. The period of the transform should be long enough to accurately compute the lowest frequencies observed in the signal. This requirement must be balanced with the computational expense of integrating the mixing layer for long times. Since the data are never strictly periodic, we must exercise caution in computing the Fourier Transforms. For sufficiently long data records windowing techniques can be used to alleviate problems with truncating the data at a finite time. Alternatively, a shorter period can be transformed by removing any offset between the first and last data point of the record. This contaminates the very low and very high frequencies in a manner similar to windowing the data. We have chosen the ladder technique, so that transforms over a relatively short period (but never less than the lowest forced frequency) can be computed. The results presented below have found to be fairly insensitive to the length of the transform so long as it is not shorter than one period of the 3rd sub-harmonic.

Figure 4 shows contours of the mean streamwise velocity of the mixing layer. The width of the layer essentially doubles at each pairing. In Figure 5, the amplitude of the temporal Fourier Transform of the streamwise velocity is plotted along the centerline of the layer ($y = 0$) for the fundamental frequency and the first two sub-harmonics. For the two sub-harmonic disturbances, a exponential growth of the instability wave is followed by saturation and eventual decay. Note that the amplitudes do not decay significantly before they enter the sponge region at $x = 285$. The fundamental disturbance reaches a 2nd peak after its original saturation, evidently due to its generation as a harmonic component of the first sub-harmonic frequency. The approximate saturation locations for the fundamental frequency, first and second sub-harmonics are $x = 50$, $x = 75$ and $x = 175$.

### *3.2 Acoustic Field*

The DNS fields away from the mixing region contain the acoustic waves produced by the layer. Using the DFT over 1 period of the 3rd sub-harmonic, as discussed in the last section, we transform the dilatation in the far-field into frequency space. The transformed dilatation was also computed with transforms of length 2 and 4 periods of the 3rd sub-harmonic, with very little qualitative difference in the results presented below. Dilatation, $\theta = \frac{\partial u}{\partial x} + \frac{\partial v}{\partial y}$ is chosen as the acoustic variable for several reasons. First, it is directly related to the acoustic pressure at large $\pm y$. In the high speed stream:

$$\frac{\partial p'}{\partial t} + M_1 \frac{\partial p'}{\partial x} = -\gamma \theta', \qquad (1)$$

For the low speed stream replace $M_1$ with $M_2$ in Equation 1. Secondly, the dilatation decays from its near field hydrodynamic values to its acoustic values away from the layer much more quickly than does the pressure.

In Figure 6, contours of the temporal Fourier Transform of the dilatation are plotted away from the sheared region for 4 different frequencies: the fundamental and

its first two sub-harmonics, and an unforced frequency half way between the fundamental and the first sub-harmonic. For reference, the maximum contour levels shown in Figure 6 are converted to their approximate pressure levels relative to the ambient pressure far from the shear layer (atmospheric pressure) in Table 1. The dilatation at a particular frequency is complex– the real part is plotted in Figure 6 (which corresponds to a particular phase). The saturation locations for the instability waves are indicated on the plot. It is evident that the acoustic waves at the fundamental frequency and its first two sub-harmonics are generated near the region where the instability waves for these modes saturate. That is, the acoustic waves at the fundamental frequency appear to emanate from the region where the vorticity rolls up into discrete vortices, and the acoustic waves at the sub-harmonics appear to emanate from the regions where the pairings occur. This is in agreement with the experiments of Laufer and Yen[11] who observed the same phenomena, and with the analysis of Crighton and Huerre[12], and Mankbadi[13], and Mankbadi and Liu[14]. In fact, it appears from the Figure that for the 1st and 2nd sub-harmonic frequencies the waves are primarily focused downstream, reaching their maximum amplitude (for a given distance from their apparent origin) near the downstream axis. In contrast with the experiments, the computations of the acoustic field at the fundamental frequency have maximum amplitude in directions nearly normal to the layer.

We have not yet attempted to make a detailed comparison with the experimentally measured fields since the computational domain is not large enough to represent the true far field where any cancellation of waves from different source locations would be complete, and because the experiments are performed in a jet (3D).

For the fundamental and first sub-harmonic frequency, spurious acoustic waves emanating from the outflow boundary (sponge region) are also evident, resulting in the choppy pattern in the waves near the outflow boundary. These spurious waves are even more striking when we examine the acoustic field at the unforced frequency, Figure 6(d). In fact, such spurious waves are found for nearly all the frequencies except those explicitly forced. However, it should be noted that the energy in these frequencies is much smaller than the energy at the forced frequencies, generating much smaller acoustic waves. therefore the resulting acoustic field is probably much smaller than that of the forced frequencies. Note that the acoustic waves at the unforced frequency shown in Figure 6(d) is roughly an order of magnitude smaller than the acoustic field at the fundamental frequency. In a more turbulent flow with larger energy at the unforced frequencies, reflections by the sponge may not dominate the acoustic field at those frequencies. However, the small presence of some reflections even in the acoustic fields of the forced frequencies indicates the need for further refinements to the downstream boundary conditions.

## 5.0 Conclusions

The sound generated by a two dimensional shear layer has been computed by solving the compressible Navier-Stokes equations. A numerical scheme has been developed which is capable of accurately computing both the near field hydrodynamics as well as the generated acoustic field, even at relatively low Mach numbers. As an indication of the range of energies the computations are able to resolve, the far field acoustic waves have velocities on the order of $10^{-5}$ compared to the mean velocities in the layer, while the near field hydrodynamic fluctuations are on the order of $10^{-1}$ compared to the mean values.

The sponge outflow developed by the current authors[4] was found to be adequate to prevent reflections from contaminating the acoustic field at only the most energetic frequencies. For other frequencies with weaker acoustic fields, reflections from the sponge outflow seriously contaminated the results. Further refinements to downstream boundary conditions are warranted for cases where acoustic waves of even smaller amplitude are to be computed.

The mixing layer was forced with the fundamental frequency and its first 3 sub-harmonics which caused the layer to become quasi-periodic in time over the entire domain of length $285\delta$ in the streamwise direction (where $\delta$ is the vorticity thickness of the layer at the inflow). The acoustic fields at the fundamental and first two sub-harmonic frequencies were found to be dominated by waves which originate near the region where the instability waves of their particular frequency saturate. That is, the acoustic waves at the fundamental frequency are radiated primarily from the region where the layer rolls up, waves at the first sub-harmonic are radiated from the region near the first pairing, and waves at the 2nd sub-harmonic are radiated from the region near the second pairing. This is in accord with the experiments of Laufer and Yen[11]. Furthermore, the waves generated by the sub-harmonics have greatest amplitude near the downstream direction, also in agreement with the experiments.

We are currently performing calculations to determine the acoustic sources in the mixing layer. In the future we will report predictions for the acoustic fields found by solving Lilley's acoustic analogy based on source

terms computed from the DNS. Such predictions will be useful in validating aeroacoustic theory for the sound generated by large scale structures in spatially developing shear flows, and in extending the acoustic field to larger distances from the source region than can be computed with DNS.

**Acknowledgements.**

This work was supported by the Office of Naval Research. Computer time was provided by NASA Ames.

**References.**

1. Kambe, T. 'Acoustic emissions by vortex motions.' *J. Fluid Mech.* Vol. 173, pp. 643-666, 1986.
2. Goldstein, M.E. 'Aeroacoustics of turbulent shear flows.' *Annual Review of Fluid Mechanics* Vol.16, pp. 263-285., 1984.
3. Lilley, G.M. 'On the noise from jets.' *AGARD* Report CP-131, 1974.
4. Colonius, T., Lele, S. K. and Moin, P. 'Boundary conditions for direct computation of aerodynamic sound.' *AIAA Journal*, Vol. 31., pp. 1574-1582, 1993.
5. Mitchell, B.E., Lele, S. K. and Moin, P. 'Direct computation of the sound from a compressible corotating vortex pair.' *AIAA paper* 92-0374, 1992. *also, to appear in J. Fluid Mech.*
6. Colonius, T., Lele, S. K. and Moin, P. 'Scattering of sound waves by a compressible vortex–numerical simulations and analytical solutions.' *to appear J. Fluid Mech.*
7. Giles, M. B. 'Nonreflecting boundary conditions for Euler equation calculations.' *AIAA J.*, Vol 12, pp. 2050–2058, 1990.
8. Lele, S.K. 'Compact finite difference schemes with spectral-like resolution.' *J. Comp. Physics*, Vol. 103, pp. 16-42, 1992.
9. Sandham, N.D. and Reynolds, W.C. 'A numerical investigation of the compressible mixing layer.' *Thermoscience Division, Department of Mechanical Engineering, Stanford University*, Report No. TF-45, 1989.
10. Ho, C.M., Zohar, Y., Foss, J.K., and Buell, J.C. 'Phase decorrelation of coherent structures in a free shear layer.' *J. Fluid Mech.*, Vol. 230, pp. 319-337, 1991.
11. Laufer, J. and Yen, T. 'Noise generation by a low-Mach-number jet.' *J. Fluid Mech.*, Vol. 134, pp. 1-31, 1983.
12. Crighton, D.G. and Huerre, P. 'Shear-layer pressure fluctuations and superdirective acoustic sources.' *J. Fluid Mech.*, Vol. 220, pp. 355-368, 1990.
13. Mankbadi, R.R. 'The self-noise from ordered structures in a low Mach number jet.' *Journal of Applied Mechanics.* Vol 157, pp. 241-246, 1990.
14 Mankbadi, R.R. and Liu, J.T.C. 'Sound generated aerodynamically revisited: Large scale structures in a turbulent jet as a source of sound.' *Phil. Trans. R. Soc. Lond. A*, Vol 311, pp 183-217, 1984.

| Frequency | Dilatation* | Pressure Level[2]** |
|---|---|---|
| $\omega_f / 4$ | $1.0 \times 10^{-6}$ | $4 \times 10^{-10}$ |
| $\omega_f / 2$ | $.4 \times 10^{-6}$ | $16 \times 10^{-10}$ |
| $\omega_f$ | $.2 \times 10^{-6}$ | $1 \times 10^{-12}$ |

* Relative to the speed of sound in the high speed stream and vorticity thickness

** Relative to the ambient pressure

TABLE 1. Approximate pressure levels corresponding to the contour levels of dilatation plotted in Figure 6.

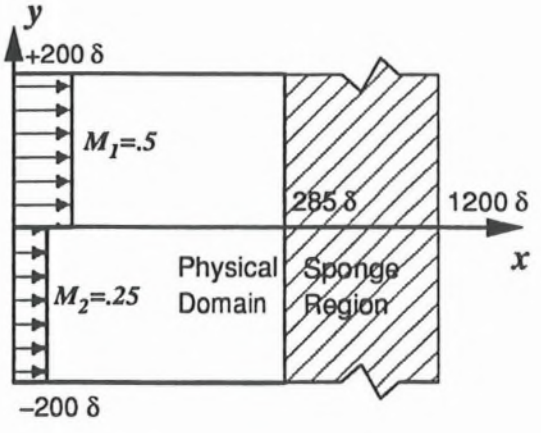


FIGURE 1. Schematic diagram of computational domain for spatially developing mixing layer.

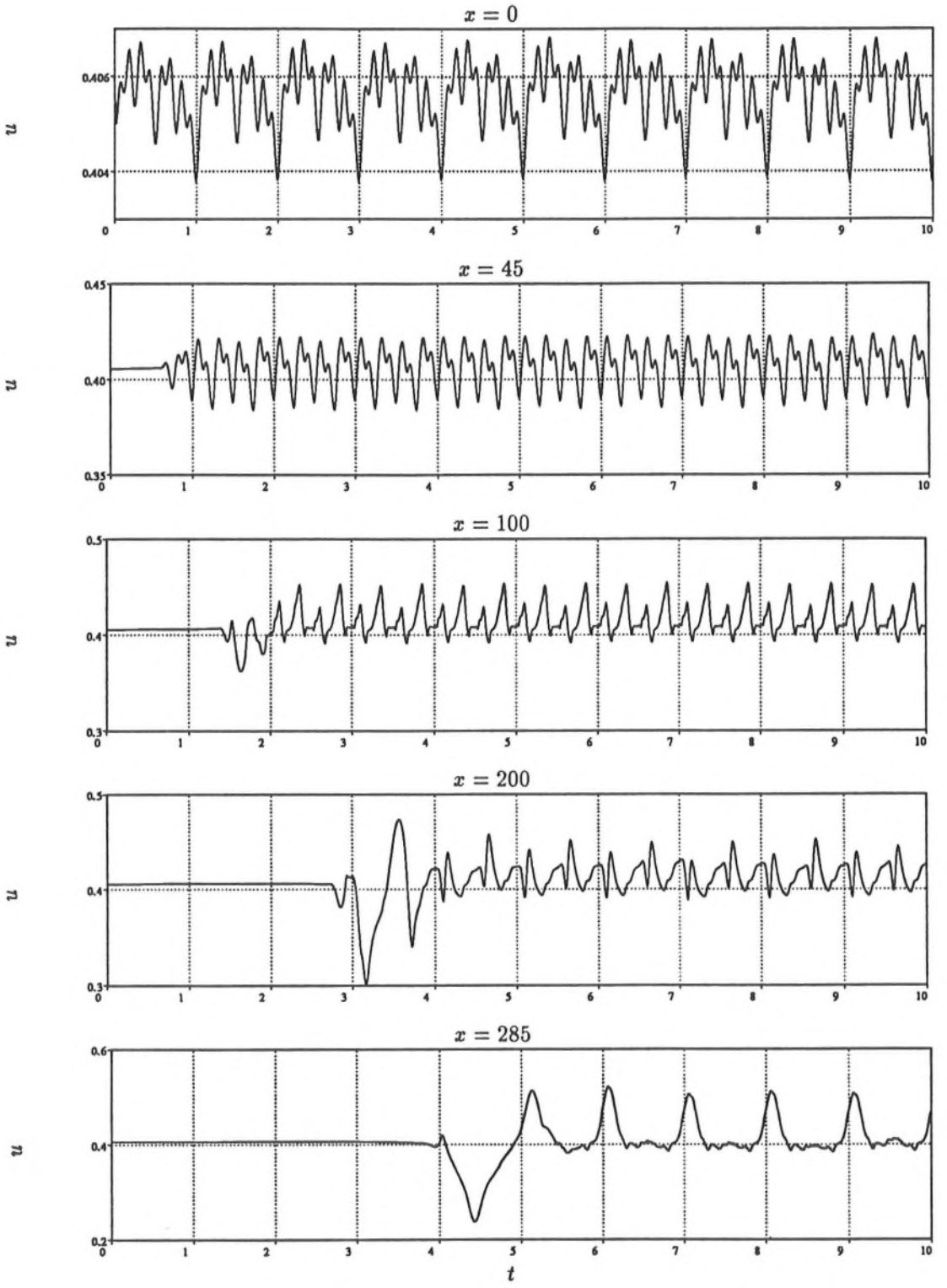


FIGURE 2. Traces of the streamwise velocity (normalized by the sound speed in the high speed stream) in time at various streamwise locations at $y = 0$. Time is normalized by the period of the 3rd sub-harmonic frequency.

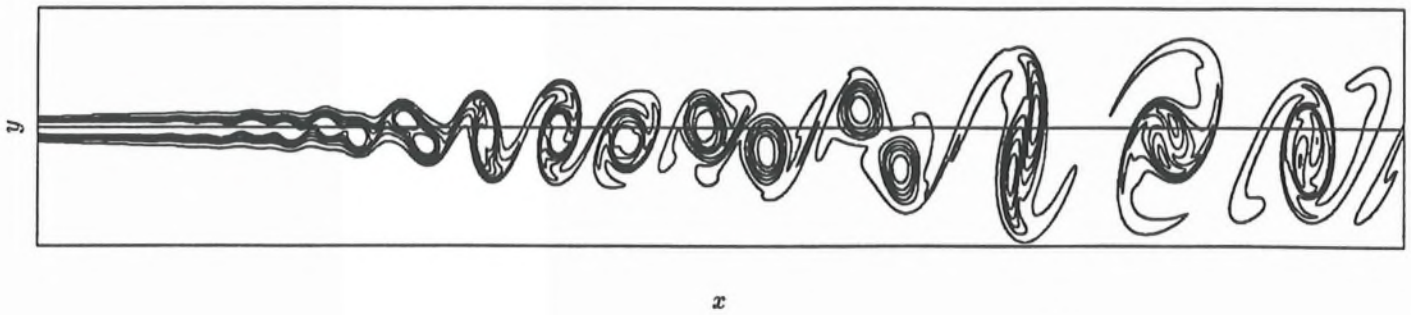


FIGURE 3. Vorticity contours in near field mixing region. The normal axis is expanded by a factor of 2.5. A small portion of the computational domain is shown which extends to $285\delta$ in the streamwise direction and $\pm 10\delta$ in the normal direction. Vorticity is normalized with the speed of sound in the high speed stream and the initial vorticity thickness. Contour levels: Min: -.13, Max: -.01,Increment: .02.

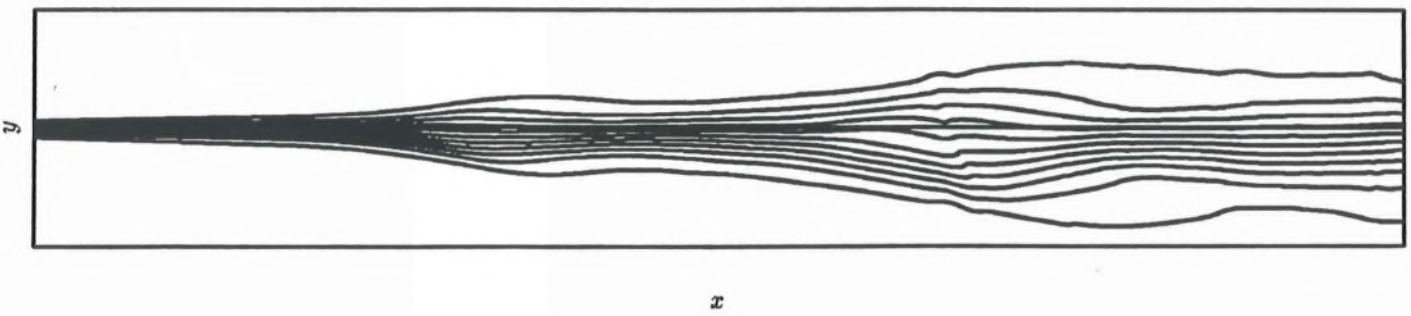


FIGURE 4. Mean streamwise velocity relative to the speed of sound in the high speed stream. The domain is the same as in Figure 3. Contour levels: Min: .26, Max: .49,Increment: .023.

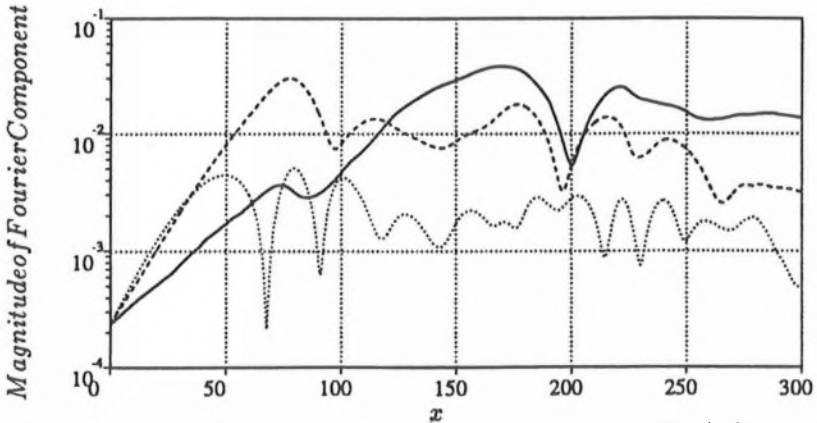


FIGURE 5. Magnitude of temporal Fourier component of the streamwise velocity (relative to the speed of sound in the high speed stream). —— 2nd sub-harmonic freq. ---- 1st sub-harmonic. ····· Fundamental.

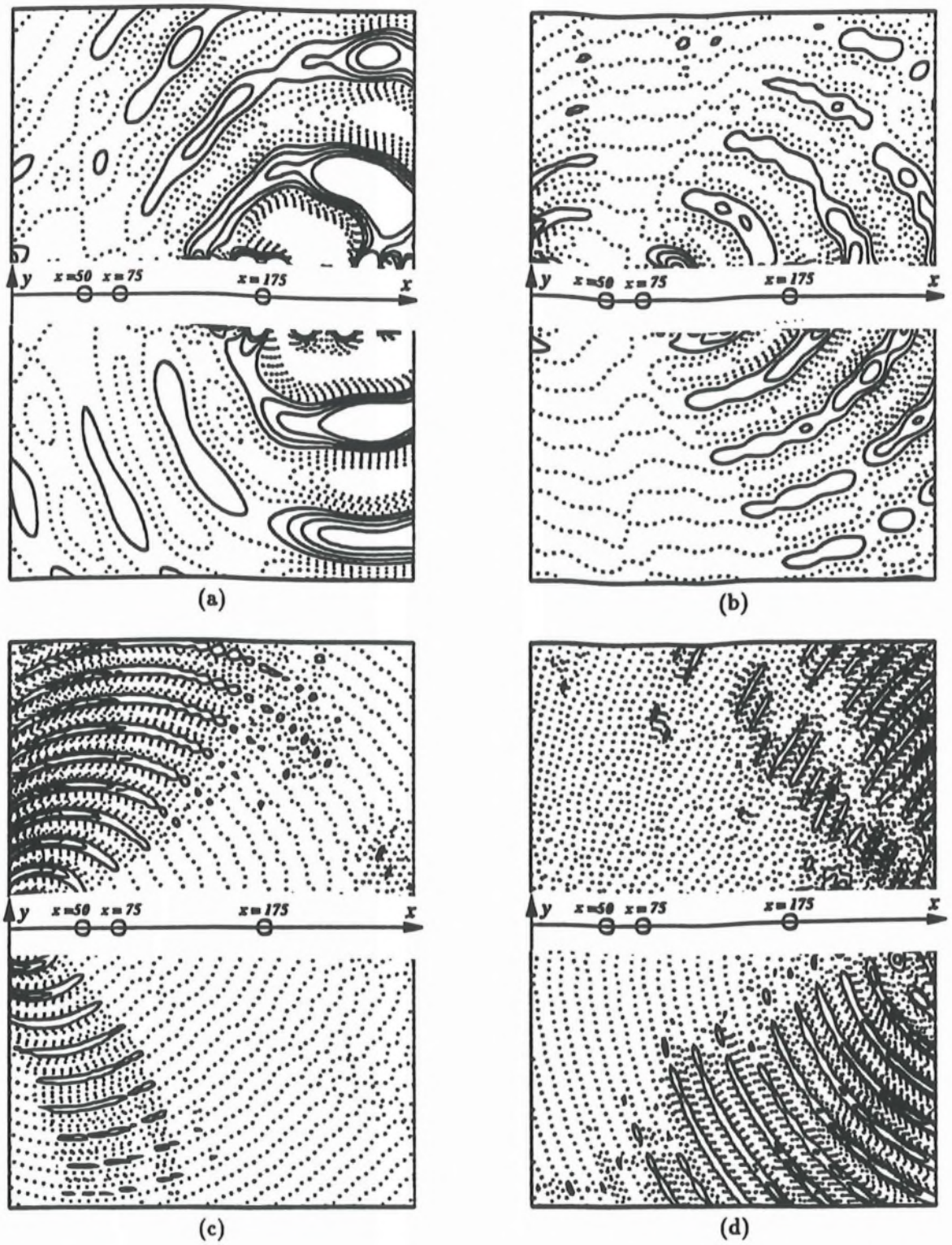


FIGURE 6. Contours of the dilatation (normalized by the sound speed in the high speed stream and the vorticity thickness) for various frequencies away from the sheared region. The part of the domain shown extends to $285\delta$ in $x$ and $\pm 200\delta$ in $y$. The circles indicate the approximate saturation locations $\omega_f$, $\omega_f/2$, and $\omega_f/4$. Dotted lines are negative contours and zero, solid lines are positive contours. (a) $\omega_f/4$, Contours: Min= $-1 \times 10^{-6}$, Max= $1 \times 10^{-6}$, Increment= $.25 \times 10^{-6}$. (b) $\omega_f/2$, Contours: Min= $-.4 \times 10^{-6}$, Max= $.4 \times 10^{-6}$, Increment= $.1 \times 10^{-6}$. (c) $\omega_f$, Contours: Min= $-.2 \times 10^{-6}$, Max= $.2 \times 10^{-6}$, Increment= $.05 \times 10^{-6}$. (d) $3\omega_f/4$, Contours: Min= $-.02 \times 10^{-6}$, Max= $.02 \times 10^{-6}$, Increment= $.005 \times 10^{-6}$. Note the much smaller contour levels in (d).